Core–Shell Microcapsules With Embedded Microactuators for Regulated Release

Haifeng Yang, Xuan Qiao, Wei Hong, and Liang Dong, *Member, IEEE*

***Abstract*—Core–shell microcapsules capable of regulating the release profile of encapsulated molecules are developed. These microcapsules uniquely embed miniature actuators in their liquid core. The internal actuators are made of stimuli-responsive smart hydrogel beads. The embedded hydrogel beads swell in response to external electric fields, regulating the internal pressure of the liquid core and thus the diffusion rate of the encapsulated molecules from the microcapsules. The incorporation of the actuators into the interior of the microcapsules provides an internal control variable to a conventional diffusion-based release process. The microcapsules, which behave much like microelectromechanical systems, are fabricated by a simple co-electrospray process. This fabrication technique allows integrating the hydrogel beads, forming the polymer shell, and loading the releasable molecules simultaneously in one step. [2012-0179]**

***Index Terms*—Controlled release, electrospray, microcapsules, stimuli-responsive hydrogel.**

I. Introduction

CONTROLLED encapsulation and release of biological and chemical agents and species (e.g., drugs, proteins, vitamins, cells, fragrances, and flavors) is of great importance to many applications, ranging from food and pharmaceutical industries to inkless paper [1]–[4]. Particularly, liquid core–polymer shell hollow microcapsules have attracted much attention. The polymer shells make microcapsules more stable and robust, not only protecting sensitive ingredients against denaturing environments but also allowing for easy handling of liquids [5]–[8]. By controlling the thickness, porosity, and/or mechanical strength of the polymer shells, it is possible to release the encapsulated ingredient in a controlled manner [9]. From the perspective of microcapsule preparations, many methods have been investigated to realize different types of hollow polymeric microcapsules such as polymersomes, multilayered capsules, and hollow microspheres. The methods include self-assembly of microgels in droplets [10], layer-by-layer polyelectrolyte deposition [11], interfacial polymerization [12], precipitation by phase separation [13], surface polymerization [14], copolymer vesicles [15], multiphase microfluidics [16], and combination of molecular self-assembly and precipitation [17]. These methods have led to substantial progress in manufacturing different kinds of hollow microcapsules but have often required relatively nontrivial and complex chemical strategies [5]. From the perspective of release mechanisms, presently, three major methods exist for releasing encapsulated ingredients out of hollow microcapsules [18], [19]. The first method involves shell rupture through applied pressure, where a critical pressure was determined by the shell material and thickness [20], [21]. The second scheme relies on dissolving the shell material by melting, enzyme attack, or chemical reaction, where molecular release over a desired period of time was realized through a slow diffusion process [22]–[24]. The last scheme uses a swellable polymer shell. The mechanical strength of the polymer shell could be tuned by external stimuli such as electric fields, pH, temperature, or biochemical reaction. This, in turn, changes the diffusion rate of the encapsulated molecules from the microcapsules [25]–[28].

Electrospinning is a popular, simple, and versatile technique to generate micro/nanofibers from a wealth of materials. It utilizes a high-strength electric field to draw a charged solution into a liquid jet from a nozzle [29]. Electrospray is similar to electrospinning, except that the ejected liquid jet breaks up into small droplets when the charged solution has low viscosity or concentration. New applications of these manufacturing techniques are continuously being developed for energy storage, catalysis, sensors, and drug delivery [9], particularly as many interesting complex micro/nanostructures (e.g., hollow interiors, core–sheath complexes, and multicompartments [9], [30]–[33]) can be realized by using modified electrospinning/spray processes (e.g., coaxial and multijet electrospinning/spray).

In this paper, we report on the development of a new class of core–shell microcapsules capable of regulating the release profile of encapsulated molecules. The uniqueness of the microcapsules laid in embedding miniature actuators into their interior [see Fig. 1(a)–(c)]. The embedded actuators were made of electrically sensitive hydrogel beads that could swell and contract by external electric fields. This allowed us to regulate the internal pressure of the liquid core and thus the diffusion rate of the encapsulated molecules from the microcapsules. Basically, changing the electric field strength applied to the embedded hydrogel beads caused redistribution of mobile ions inside the beads. This led to imbalanced osmotic pressure and thus the swelling of the hydrogel beads [34]. It is believed that the hydrogel beads had a positive excess volume: The total volume of the hydrogel beads–solution system of the

Manuscript received June 26, 2012; revised October 7, 2012; accepted November 5, 2012. Date of publication November 29, 2012; date of current version May 29, 2013. This work was supported in part by the National Science Foundation under Grant ECCS-1102354 and in part by the Wagner-McGee Interdisciplinary Research Fund. Subject Editor X. Zhang.

H. Yang, X. Qiao, and L. Dong are with the Department of Electrical and Computer Engineering, Iowa State University, Ames, IA 50011 USA (e-mail: ldong@iastate.edu).

W. Hong is with the Department of Aerospace Engineering, Iowa State University, Ames, IA 50011 USA.

Color versions of one or more of the figures in this paper are available online at http://ieeexplore.ieee.org.

Digital Object Identifier 10.1109/JMEMS.2012.2227950

1057-7157/$31.00 © 2012 IEEE

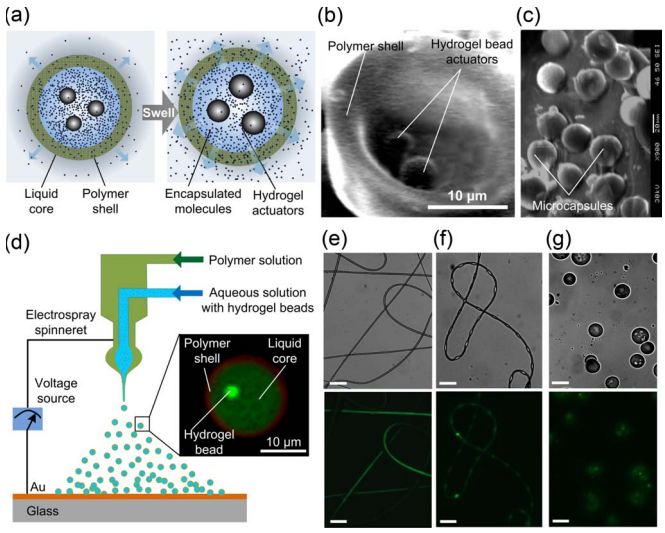

Fig. 1. (a) Schematic structure and mechanism of the liquid core–polymer shell microcapsule for regulated release of encapsulated molecules. The microcapsule contains electrically sensitive hydrogel beads in its liquid core. The hydrogel beads expand by external electric fields. This causes the internal pressure of the liquid core to increase, regulating the release of the encapsulated molecules. (b) SEM image of an opened microcapsule showing the hydrogel beads. (c) SEM image of the microcapsules produced by co-electrospray. (d) Schematic setup of co-electrospray for fabricating the microcapsules embedding hydrogel beads. The inset shows a fluorescent image of a microcapsule containing a hydrogel bead. (e)–(g) Morphological transition of co-electrospray products, obtained by adjusting the PDLA-to-chloroform WR used for the outer flow of the polymer solution. (e) Continuous core–shell fibers with WR $= 1 : 8$. (f) Beaded fibers with WR $= 1 : 10$. (g) Independent core–shell microcapsules with WR $= 1 : 15$. The scale bars in (e)–(g) represent 20 μm. The drawings in (a) and (d) are not to scale.

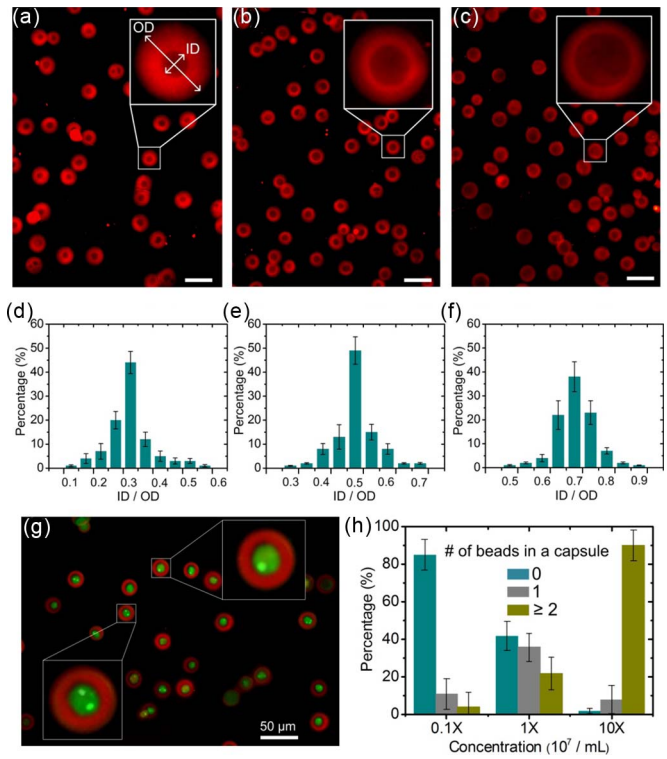

Fig. 2. (a)–(c) Fluorescent images showing the liquid core–polymer shell microcapsules without hydrogel beads, fabricated at inner flow rates of 0.08, 0.4, and 0.8 mL/h, repectively. The outer flow rate was fixed at 8 mL/h. No hydrogel beads were introduced to the inner flow during the electrospray process. The scale bars represent 50 μm. (d)–(f) Histograms of the ratio of the ID to the OD (ID/OD) for the corresponding microcapsules shown in the same columns in (a)–(c). (g) Fluorescence image showing the liquid core–polymer shell microcapsules with embedded hydrogel beads. Here, the concentration of the hydrogel beads that used the inner flow of the electrospray process was $C_{\text{bead}} = 2 \times 10^7/\text{mL}$. The flow rate of the inner flow was 0.4 mL/h. The bright green spots indicate hydrogel beads. The red annular rings indicate the PDLA shells. (h) Histogram of the number of the hydrogel beads observed inside the microcapsules when (left) $C_{\text{bead}} = 2 \times 10^6/\text{mL}$, (middle) $C_{\text{bead}} = 2 \times 10^7/\text{mL}$, and (right) $C_{\text{bead}} = 2 \times 10^8/\text{mL}$.

microcapsules increased when more water was imbibed in the hydrogel network [35]. The excess volume increased the internal pressure of the microcapsule, thinned the polymer shell (and possibly increased its permeability), and thus regulated the releasing flux of the encapsulated molecules. Therefore, the embedded actuators provided an internal control variable to a conventional diffusion-based molecule release process, making it possible to regulate the release characteristic of the encapsulated molecules from the microcapsules. The microcapsules had the microelectromechanical systems (MEMS)-like structures and functions [36] and were manufactured by the coaxial electrospray or co-electrospray process [37]. This technique allowed us to integrate the hydrogel beads, form the polymer shell, and load the releasable molecules in a single step.

II. Experimental

A. Co-Electrospray and Process Conditions

Fig. 1(d) shows the co-electrospray setup for fabricating the microcapsules. As a critical component, a coaxial spinneret was formed by inserting a 21-guage needle into a 23-guage needle (BD Biosciences). The spinneret allowed the delivery of the inner and outer flows independently by two individual syringe pumps (KDS 2000, KD Scientific). The outer flow contained a polymer solution for forming the shell of the microcapsules. The inner flow contained an aqueous solution of hydrogel beads and releasable molecules of interest. A high voltage (Gamma High Voltage Research) was applied between the spinneret and a collector. The collector was a grounded conductive substrate (a gold-coated glass cover slip). For all of the co-electrospray experiments, the voltage of $V_{\text{sc}} = 9.5$ kV was applied between the spinneret and the collector with a distance of 10 cm [see Fig. 1(d)]. The co-electrospray setup was located in a chemical hood at room temperature ($\sim$23 °C) and relative humidity of $\sim$45%.

In the study of forming independent hollow microcapsules [see Fig. 1(e)–(g)], the flow rate for delivering the outer Poly(D-lactic acid) (PDLA, MW $= 41\,000$, Lactel Polymers) solution (solvent: chloroform, Sigma-Aldrich) and the inner aqueous solution was adjusted to be $\text{FR}_{\text{outer}} = 8$ mL/h and $\text{FR}_{\text{inner}} = 0.4$ mL/h, respectively. The PDLA-to-chloroform weight ratio (WR) of the precursor polymer solution was changed from 1 : 8 to 1 : 15. In the study of tuning the inner diameter (ID) and outer diameter (OD) of the microcapsules [see Fig. 2(a)–(f)], the FR_{inner} was varied from 0.08 to 0.8 mL/h, whereas the FR_{outer} was fixed at 8 mL/h with WR $= 1 : 15$. In the experiment of examining the statistical distribution of hydrogel beads inside the microcapsules [see Fig. 2(h)], $\text{FR}_{\text{inner}} = 0.4$ mL/h

and $FR_{outer} = 8$ mL/h. Similarly, the microcapsules used in Figs. 4 and 5 for testing the controlled molecule release were formed at $FR_{inner} = 0.4$ mL/h and $FR_{outer} = 8$ mL/h. The concentration of hydrogel beads in the inner aqueous solution was $2 \times 10^7/\text{mL}$, which was measured by flow cytometry (FACSAria III, BD Biosciences). To study the influence of the shell thickness of microcapsules on their release characteristic [see Fig. 6(a)], three microcapsule samples with different shell thicknesses and the same hydrogel bead concentration $(2 \times 10^7/\text{mL})$ were prepared at $FR_{inner} = 0.08$, 0.4, and 0.8 mL/h, respectively. FR_{outer} used in this study was 8 mL/h. To study the influence of the quantity of hydrogel beads on the release characteristic of microcapsules [see Fig. 6(b)], two microcapsule samples were prepared with the same inner and outer flow rates of $FR_{inner} = 0.4$ mL/h and $FR_{outer} = 8$ mL/h but with different bead concentrations of $2 \times 10^7/\text{mL}$ and $2 \times 10^8/\text{mL}$, respectively.

B. Polymer Shell and Liquid-Core Materials

The PDLA solution was used as the outer flow of the co-electrospray process. The hydrophobic property of PDLA satisfied a prerequisite for encapsulating aqueous liquids into a polymer shell using co-electrospray [38]–[40]. PDLA precursor solutions with different concentrations were prepared by mixing PDLA pellets (MW = 41 000, Lactel Polymers) and chloroform (Sigma-Aldrich) in appropriate WRs. The solutions were stored at 4 °C for 24 h to dissolve these pellets and then stirred at room temperature to obtain a transparent homogeneous solution.

Deionized (DI) water containing hydrogel beads and releasable molecules were used as the inner flow of the co-electrospray process. Ten-milligram brilliant blue G (BBG) dyes were mixed into 10-mL DI water and then stirred at room temperature to obtain the BBG solution with the concentration of 1 mg/mL.

C. Preparation of Electrically Sensitive Hydrogel Beads

There are a lot of different available hydrogels sensitive to different external stimuli such as infrared light [41], visible light [42], ultrasound [43], temperature [35], and magnetic fields [44]. Here, in this work, a homemade electrically sensitive hydrogel was used as a model hydrogel. The diameter of the hydrogel beads was 3.2 ± 2.1 μm (the mean $\pm$ standard deviation obtained from ~200 hydrogel beads). Different hydrogel bead suspensions were prepared, with the bead concentration C_{bead} ranging from 2×10^6 to $2 \times 10^8/\text{mL}$.

The hydrogel precursor solution was formed by mixing acrylic acid (Sigma-Aldrich) and 2-hydroxyethyl methacrylate (Sigma-Aldrich) in a molar ratio of 1 : 4.2, ethylene glycol dimethacrylate (1.2 wt%, Sigma-Aldrich) and 2, 2-dimethoxy-2-phenyl-acetophenone (1.9 wt%, Sigma-Aldrich). The preparation procedures for the electrically sensitive hydrogel beads were described here.

1) The prepared hydrogel precursor solution was mixed with light mineral oil (NF/FCC, Fisher Scientific) in a volume ratio of 1 : 1.
2) The mixture was stirred by a vortex mixer (2000 r/min; Fisher Scientific) for 20 s and then exposed under ultraviolet (UV) irradiation (intensity: 27.5 mW/cm^2) for 20 s.
3) After the stirring and UV exposure steps in (2) were repeated for six times, a mixture of hydrogel beads and mineral oil was obtained.
4) To separate the hydrogel beads from the mineral oil, the mixture (3 mL) was added to 2-mL methanol (Sigma-Aldrich) in a vial and then agitated in an ultrasonic mixer (B2510-MT, Branson) for 5 min.
5) After the resultant mineral oil droplets deposited on the bottom of the vial, the mixture of the methanol and hydrogel beads was taken by a pipette and then put in a new vial.
6) To separate the methanol from the hydrogel beads, the mixture was centrifuged in the new vial at 1000 r/min for 5 min.
7) After the upper methanol was thrown away, chloroform (2 mL; Sigma-Aldrich) was added to the vial, to remove the remaining mineral oil droplets.
8) After the chloroform evaporated away, methanol (2 mL) was added again to resuspend the hydrogel beads.
9) After the mixture was centrifuged at 1000 r/min for 5 min, the upper methanol was thrown away.
10) The hydrogel beads (diameter: 3.2 ± 2.1 μm) were finally obtained after dried in air.

D. SEM Imaging and Fluorescence Microscopy

A SEM (S-2460N, Hitachi) was used to examine the hydrogel beads embedded inside the microcapsules [see Fig. 1(b)] and the morphology of the microcapsules [see Fig. 1(c)]. To open a typical microcapsule shown in Fig. 1(b), a tungsten probe was first treated with chloroform and then carefully contacted the outer surface of the microcapsule for ~5 s under a stereo microscope. Finally, the sample was dried on a hotplate at 50 °C for ~1 min.

A fluorescence microscope (DM 4500B, Leica) was used to visualize the PDLA polymer shell and the embedded hydrogel beads of the microcapsules. A small amount of Rhodamine B (pure, MW = 479, Sigma-Aldrich) and fluorescein (pure, MW = 332.3, Sigma-Aldrich) dye powders was added to the PDLA and hydrogel precursor solutions, respectively, to obtain the red fluorescence in Fig. 2(a)–(c) and the merged red and green fluorescence in Fig. 2(g) and in the inset in Fig. 1(d). An exception was in Fig. 1(e), where a small amount of fluorescein dye powders was added into the PDLA precursor solution to obtain the green fluorescence.

III. RESULTS

A. Co-Electrospray of Core–Shell Microcapsules

The concentration of the PDLA polymer solution was first optimized to form independent hollow microcapsules by the co-electrospray process. Here, $FR_{outer} = 8$ mL/h and $FR_{inner} = 0.4$ mL/h. As the relative amount of PDLA with respect to the solvent (chloroform) decreased, the morphology of the co-electrospray products was found to change from a fibrous to a spherical form. Fig. 1(e) and (g) shows the continuous

core–shell microfibers and independent hollow microspheres formed with the critical PDLA-to-chloroform WRs of WR $=$ $1:8$ and $1:15$, respectively. When the WR fell between these two critical ratios, the beaded fibrous structures [see Fig. 1(f)] were emerged. When the WR $<1:18$, the PDLA polymer solution was too thin to wrap the inner liquid, which flowed out of the spinneret and fell onto the collector.

It was possible to tune the ID of the microcapsules by adjusting the flow rate of the inner flow $\mathrm{FR_{inner}}$. In this experiment, the WR of the PDLA solution was chosen to be $1:15$. The $\mathrm{FR_{inner}}$ was varied from 0.08 to 0.8 mL/h, whereas the $\mathrm{FR_{outer}}$ was fixed at 8 mL/h. The upper limit of the $\mathrm{FR_{inner}}$ was set to be 0.8 mL/h because, above this limit, the jetted inner flow separated from the outer flow at the tip of a two-fluid Taylor cone. Fig. 2(a)–(c) shows that increasing the $\mathrm{FR_{inner}}$ ($\leq$ 0.8 mL/h) had little influence on changing the OD (27.35 ± 2.2 μm) of the microcapsules (here, no hydrogel beads were introduced to the inner flow of the electrospray process). This was because the change of the $\mathrm{FR_{inner}}$ did not significantly affect the total flow rate of the two fluids. However, it was obvious that increasing the $\mathrm{FR_{inner}}$ gave rise to an increased ID of the microcapsules. Specifically, when the $\mathrm{FR_{inner}}$ was at 0.08, 0.4, and 0.8 mL/h, the resultant IDs were found to be 8.1 ± 2.4 μm, 16.5 ± 3.5 μm, and 19.1 ± 3.8 μm, respectively. In the succeeding discussions, each measurement for the ID, OD, and shell thickness T_{shell} of the microcapsules was the mean $\pm$ standard deviation from $\sim$200 microcapsules (the ID and T_{shell} were obtained based on their fluorescent images, and the OD was obtained based on their optical images).

We investigated controlling the quantity of hydrogel beads inside the microcapsules. By mixing a desired concentration of the hydrogel beads into the inner flow of the co-electrospray process, it was possible to obtain a statistical distribution of the number of the hydrogel beads encapsulated within the microcapsules. Basically, the encapsulation of hydrogel beads into the microcapsules was a stochastic process following the Poisson distribution function given by the formula $f(\lambda, k) = \lambda^k \exp(-\lambda)/(k!)$, where f is the probability of having k beads in a microcapsule, given an average loading number of λ beads per microcapsule [45], [46]. Let us assume that the microcapsules have the ID of 16.5 μm (the experimental mean value). Theoretically, when $\lambda = 0.1$ ($C_{\mathrm{bead}} = 2 \times 10^6$/mL), 9.05% of the microcapsules have 1 bead and 0.47% have $\geq$2 beads, whereas 90.48% contain no beads. When $\lambda = 1$ ($C_{\mathrm{bead}} = 2 \times 10^7$/mL), the possibilities for a microcapsule to contain 0, 1, and $\geq$2 beads are 36.79%, 36.79%, and 26.42%, respectively. When $\lambda = 10$ ($C_{\mathrm{bead}} = 2 \times 10^8$/mL), the possibility for one microcapsule to have $\geq$2 beads increases to be more than 99%. Fig. 2(g) shows the fluorescent image of the microcapsules (ID $= 16.5 \pm 3.5$ μm) with embedded hydrogel beads ($C_{\mathrm{bead}} = 2 \times 10^7$/mL; $\mathrm{FR_{inner}} = 0.4$ mL/h). Fig. 2(h) shows the histogram of the number of hydrogel beads observed inside the microcapsules ($C_{\mathrm{bead}} = 2 \times 10^7$/mL). The statistical distribution of the hydrogel beads in the microcapsules was obtained by counting the hydrogel beads in $\sim$500 microcapsules based on their fluorescent images. The experimental result was almost in agreement with the theoretical result estimated by the Poisson distribution formula.

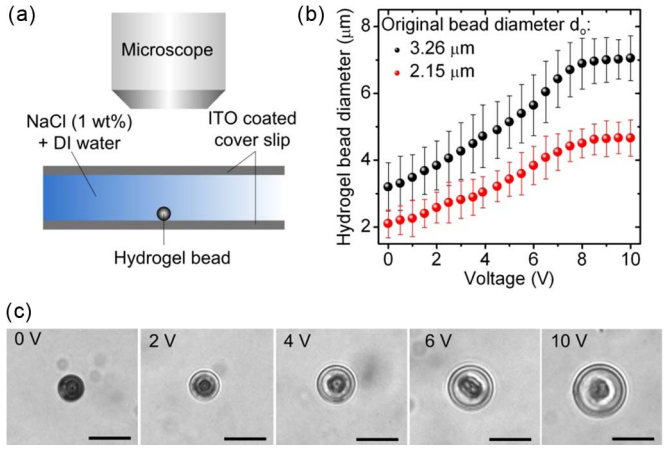

Fig. 3. (a) Experimental setup for measuring the swelling characteristic of an electrically sensitive hydrogel bead. (b) Size responses of two hydrogel beads as a function of an applied dc voltage. A low voltage was applied and remained on for 5 min and then off for 5 min before switching to a high voltage application. (c) Final morphologies of the hydrogel bead with the original diameter of 3.26 μm under different voltage conditions. The scale bars represent 5 μm.

B. Swelling Characteristic of Electrically Sensitive Hydrogel Beads

The swelling characteristic of the hydrogel beads was measured by exposing them to different electric fields. The hydrogel beads were placed in a microfluidic chamber containing DI water with 1 wt% NaCl. The chamber was formed between two glass slides with conductive indium tin oxide (ITO) coatings. The separation distance between the two glass slides was set to be 5 mm (determined by the thickness of a homemade aluminum spacer used here). The shape change of the hydrogel beads was observed by a phase contrast microscope (DM2500, Leica) [see Fig. 3(a)]. Different dc voltages (from 0.5 to 10 V with a step of 0.5 V) were applied between the two ITO glass slides. Here, a low voltage was applied and remained on for 5 min and then off for 5 min before switching to a high-voltage application. It is noted that we applied the voltage in such a way that allowed for a precise characterization of the swelling property of the homemade electrically sensitive hydrogel beads. Our experiments showed that, after the hydrogel beads (3–5 μm in diameter) were exposed to an electric field, the time for the beads to reach a stable swollen state was 1–2 min. Thus, we applied a voltage for a time period of 5 min, which was sufficient enough to get a stable bead size. Subsequently, the voltage source was off for another time period of 5 min, which could allow the expanded beads to switch back to their original size before a new voltage application came. The swelling characteristic of the hydrogel beads when voltages were applied from high to low remained the same as that when voltages were applied from low to high.

Fig. 3(c) displays the expanded state of a hydrogel bead (original diameter: $\sim$3.26 μm) under different voltage applications. We found that it took $\sim$15 s from a voltage application to an obvious expansion of the hydrogel bead and then $\sim$18 s for the bead to reach a stable size. The response time was found to be independent of the applied voltage. This was because the movement of ions and water into and out of the hydrogel was mainly determined by diffusion, and the timescales for

dimensional change depended on the size of the hydrogel structure. Fig. 3(b) shows the dimension responses of two different-sized hydrogel beads (original diameters: 3.26 and 2.15 μm) as a function of an applied voltage. The size of the hydrogel bead reached an almost saturation value when the applied voltage was greater than 8 V. We note that, using the concentration of NaCl (1 wt%), it could be estimated that the Debye length in the solution was on the order of nanometers. Because the double layers on the water–electrode interface were much smaller than the diameter of hydrogel beads, their effect could be neglected. With the electrolysis voltage ($\sim$1.5 V) deducted, the effective electric field in water is approximately 1.7 V/mm when 10 V is applied on the 5-mm gap. The data presented in Fig. 3(b) were the mean $\pm$ standard deviation obtained from ten measurements on each hydrogel bead.

C. Controlled Release of Encapsulated Molecules From Core–Shell Microcapsules

To demonstrate the controlled release of encapsulated molecules from the microcapsules, dye BBG (1 mg/mL) was mixed with DI water containing 1 wt% NaCl. The NaCl supplement was used to provide enough mobile ions when dissociated in water. A stock hydrogel bead suspension was differently diluted with the BBG-NaCl solution to obtain a desired C_{bead} for the inner flow of the co-electrospray process. To obtain enough microcapsules for test, the co-electrospray process was conducted for 2 h. The overall loading efficiency of the BBG molecules into the microcapsules was almost 100% as the BBG solution was directly injected into the inner capillary of the spinneret by a syringe pump. The microcapsules were collected by the aforementioned gold-coated cover slip (1 cm^2). The collector served as the anode of an electric simulation unit shown in the inset in Fig. 4(a). Although a thin layer of polymer was splashed on the surface of the gold-coated cover slip below the microcapsules, it is believed that this layer had little influence on the release characteristic of the microcapsules due to its small thickness (5–10 μm) compared with the large thickness of the microcapsule layer (1.2- to 1.3-mm thick; co-electrospray time: 2 h). Thus, the microcapsules were not removed from the cover slip in the following experiments. The other gold-coated glass slide (cathode) was placed 5 mm away from and parallel to the collector. The two electrodes were immersed in a 1-mL quartz cuvette (BrandTech Scientific) containing DI water. The cumulative amount of molecule release was measured by monitoring the absorbance at the characteristic absorption wavelength of molecules (for BBG, this is 600 nm) with a spectrometer (2800 UV/Vis, UNICO). Prior to each measurement, the liquid in the cuvette was gently stirred by a glass rod to form a uniform distribution of BBG throughout the cuvette. In the following experiments, without special notification, each measurement presented in Fig. 4(b)–(g), 5, and 6 was the mean $\pm$ standard deviation from 15 samples, with each sample formed by the electrospray process for 2 h.

It was found that, as we increased the applied dc voltage to the microcapsules (ID $= 16.5 \pm 3.5$ μm; $T_{\mathrm{shell}} = 5.1 \pm 2.8$ μm; $C_{\mathrm{bead}} = 2 \times 10^7/\mathrm{mL}$), the cumulative release of BBG molecules from the microcapsules increased [see Fig. 4(a) and (b)]. Here, each sample of the microcapsules was tested under an applied voltage at a specific value. The upper limit of voltage was set to be 10 V to prevent hydrolysis. Fig. 4(a) shows the absorbance spectra of BBG molecules for different applied voltages, which were measured 2 h after each voltage application. The increase in the absorbance peak intensity at the wavelength of 600 nm indicated that the BBG release increased with increasing applied voltage. Fig. 4(b) summarizes and plots the BBG release as a function of the applied voltages. Interestingly, when the applied voltage was less than 8 V, the BBG release increased almost linearly with the voltage [see Fig. 4(b)]. However, at the higher voltages, the increasing rate of the BBG release, with respect to the voltage, decreased toward saturation. The explanation to this changing tendency is that the swelling of the hydrogel beads approached to an upper limit when exposed to the high electric fields, as shown in Fig. 3(b).

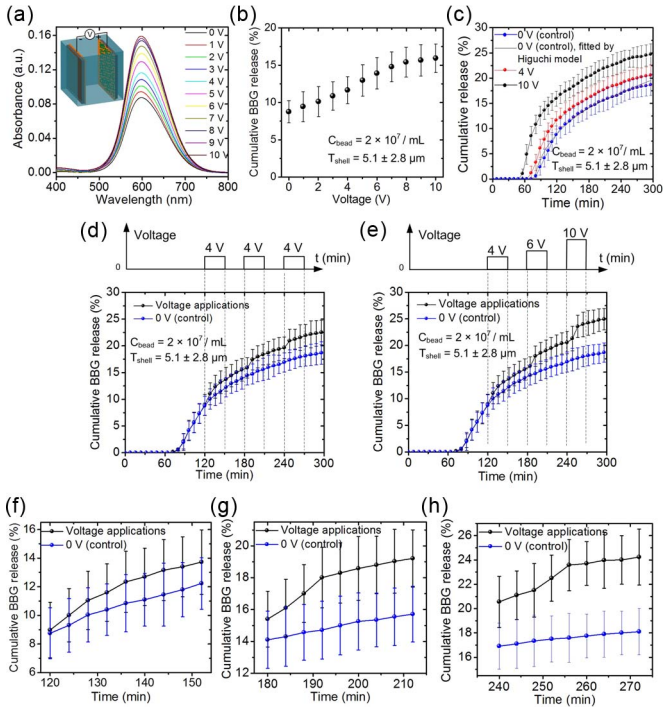

Fig. 4. (a) Absorbance spectra of BBG molecules released from ten identical samples of the microcapsules (ID $= 16.5 \pm 3.5$ μm; $T_{\mathrm{shell}} = 5.1 \pm 2.8$ μm; $C_{\mathrm{bead}} = 2 \times 10^7/\mathrm{mL}$) under different dc voltage conditions. A specific dc voltage was applied to a sample. All measurements were conducted 2 h after the voltage application. The inset shows an electric stimulation unit. (b) Cumulative BBG release from the samples measured in (a) as a function of the applied dc voltage. (c) Transient responses of three identical samples of the microcapsules to different dc voltages, namely, 0 (control), 4, and 10 V. The black curve is obtained by fitting the Higuchi model to the BBG release data of the control sample. (d) and (e) Cumulative BBG release from two identical samples of the microcapsules (ID $= 16.5 \pm 3.5$ μm; $T_{\mathrm{shell}} = 5.1 \pm 2.8$ μm; $C_{\mathrm{bead}} = 2 \times 10^7/\mathrm{mL}$), responding to two different applied square voltages. The form of the applied square voltages is shown above the release profile. (f)–(h) Magnified plots showing the details of the BBG release in (e) under three different square voltages applied at (f) $t = 120$ min, (g) $t = 180$ min, and (h) $t = 240$ min, respectively.

The transient responses of the microcapsules (ID $= 16.5 \pm 3.5$ μm; $T_{\mathrm{shell}} = 5.1 \pm 2.8$ μm; $C_{\mathrm{bead}} = 2 \times 10^7/\mathrm{mL}$) were measured to investigate the release kinetics of the microcapsules under different voltage applications [see Fig. 4(c)]. Three identical samples were tested. Two of the samples were

measured by applying the dc voltages of 4 and 10 V, respectively, at time $t = 0$. Another sample served as the control sample with no applied voltage, providing the background molecule release from the microcapsules. As shown in the control experiment result [see the blue dotted plot in Fig. 4(c)], the initial release from the sample was detected by the spectrometer at $t = 80$ min (representing the diffusion time of BBG molecules through the shell of the microcapsules). The cumulative release increased with time, whereas the increasing rate of release gradually decreased. We noted that the release characteristic of the control sample was fitted well by the Higuchi diffusion model ($Q \cong A\sqrt{t}$, where Q is the cumulative release, and A is the geometrical parameter) [47]. In contrast, the application of 4 V caused an earlier initial molecule release occurring at $t = 72$ min (8 min earlier than the control sample). As the applied voltage increased up to 10 V, the initial release occurred at $t = 56$ min, which is 24 min earlier than the control sample. By comparing the cumulative release of the microcapsules for the different applied voltages, we found that, in the period of ~40 min after the initial release, the cumulative release rose faster with the high voltage than it did with the low voltage (see the slope of each plot). Specifically, at the applied voltages of 0 (control sample), 4, and 10 V, the cumulative releases were $8.7 \pm 1.3\%$, $10.4 \pm 1.6\%$, and $13.1 \pm 1.7\%$, respectively, which were measured 40 min after their respective initial release ($t = 120$, 112, and 96 min). This provided quantitative evidence that the embedded hydrogel actuators not only triggered an earlier initial release but also enhanced the release rate in a few dozen minutes (~40 min) after the initial release. The higher the voltage applied, the earlier the initial release observed and the more molecules released within that period. This result was consistent with our observation in Fig. 3(b) that applying a higher voltage increased the volume of the embedded hydrogel beads. We note that the regulation of the release profile was effective in a few dozen minutes (~40 min) after the initial release. Afterward, the molecule release with the applied voltage progressed in a similar way to the background release from the control sample [see Fig. 4(c)]. The explanation of this result is that, as some of the encapsulated molecules were released from the microcapsules, the elevated internal pressure gradually reduced, and thus, the molecule diffusion became a dominating release mechanism. Nevertheless, the result demonstrated that the microcapsules were capable of regulating the release profile of the encapsulated molecules by changing the internal pressure to influence the regular diffusion-based release (background release).

Fig. 4(d)–(e) demonstrates tuning the release profile of the microcapsules (ID $= 16.5 \pm 3.5$ μm; $T_{\text{shell}} = 5.1 \pm 2.8$ μm; $C_{\text{bead}} = 2 \times 10^7$/mL) by applying multiple electrical stimulations at different time instances. Specifically, the first sample was tested by applying identical square voltages (amplitude $V_{\text{amp1,2,3}} = 4$ V; duration time $t_{\text{dur1,2,3}} = 30$ min) at $t = 2$, 3, and 4 h, giving rise to the net releases of $2.15 \pm 0.21\%$, $2.24 \pm 0.27\%$, and $2.17 \pm 0.24\%$, respectively [see the three steps on the black dotted plot in Fig. 4(d)]. Thus, the sample released almost equal amounts of BBG under the same voltage conditions at different time points, and the resulting release profile (the black dotted plot) deviated from the background release profile (the blue dotted curve). In the second experiment, three different square voltages with increasing amplitude ($V_{\text{amp1}} = 4$ V, $V_{\text{amp2}} = 6$ V, and $V_{\text{amp3}} = 10$ V; $t_{\text{dur1,2,3}} = 30$ min) were applied to the sample at $t = 2$, 3, and 4 h, resulting in the net releases of $2.15 \pm 0.21\%$, $2.69 \pm 0.22\%$, and $3.37 \pm 0.24\%$, respectively [see Fig. 4(e)]. Thus, the higher the amplitude of the voltage, the more the BBG release occurred. To demonstrate the possibility of realizing broad-range tuning of the release profile from the background release, we applied ten identical square voltages at different time points to the same type of the microcapsules. As shown in Fig. 5, these square voltages had the same amplitude of 10 V and the same time duration of 30 min. It was observed that each electrical stimulation triggered almost the same amount of net molecule release at ~3.4% [see the ten steps on the plot in Fig. 4(d)]. This allowed us to regulate the release profile of the microcapsules with relatively good accuracy. After the ten electrical stimulations, the resultant cumulative release was $65.2 \pm 2.19\%$, whereas the background cumulative release was only $32 \pm 1.82\%$. Thus, it was possible to realize a wide-range regulation of the release profile by applying multiple electrical stimulations to the microcapsules.

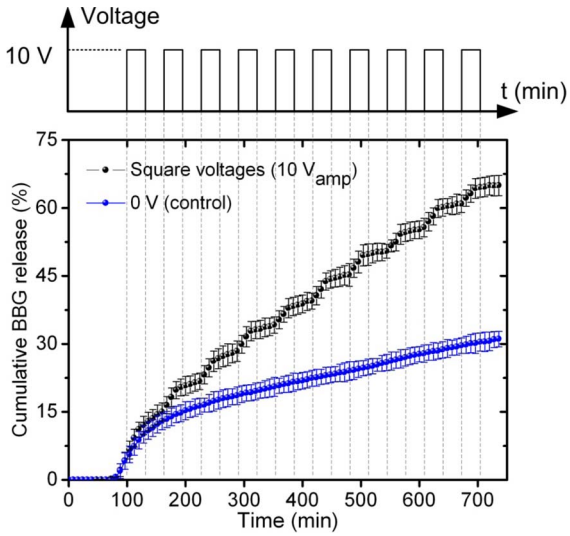

Fig. 5. Cumulative BBG release of the sample of the microcapsules (ID $= 16.5 \pm 3.5$ μm; $T_{\text{shell}} = 5.1 \pm 2.8$ μm; $C_{\text{bead}} = 2 \times 10^7$/mL) under ten identical square voltage applications with the amplitude of 10 V and the duration of 30 min.

To investigate how the shell thickness T_{shell} of the microcapsules influenced the molecule release, three different samples (named samples S_1, S_2, and S_3) were prepared with shell thicknesses of $T_{\text{shell-S1}} = 3.2 \pm 2.1$ μm, $T_{\text{shell-S2}} = 5.1 \pm 2.8$ μm, and $T_{\text{shell-S3}} = 9.1 \pm 2.5$ μm, respectively (note that $T_{\text{shell-S1}} < T_{\text{shell-S2}} < T_{\text{shell-S3}}$). The OD of the microcapsules in these samples was the same at 27.35 ± 2.2 μm. The concentration of the hydrogel beads used for all three samples was also the same at $C_{\text{bead}} = 2 \times 10^7$/mL. The dc voltage of 6 V was applied to the samples at $t = 0$. Fig. 6(a) demonstrates that decreasing T_{shell} caused an earlier initial release from the microcapsules. Specifically, the initial release times of samples S_1, S_2, and S_3 were found to be $t_{S1} = 40$ min, $t_{S2} = 48$ min, and $t_{S3} = 64$ min, respectively. However, it is

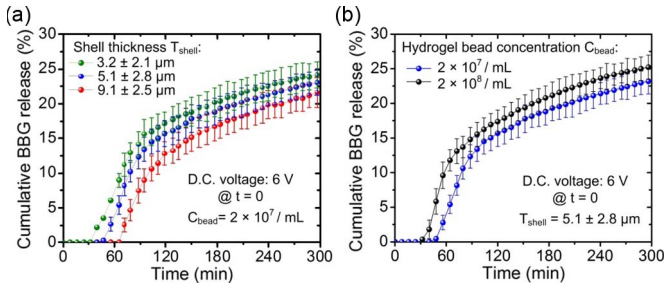

Fig. 6. (a) Cumulative BBG release of three different samples. The samples were differentiated from each other by the shell thickness of the microcapsules (listed in the plot). OD $= 27.35 \pm 2.2$ μm. $C_{\rm bead} = 2 \times 10^7$/mL. The dc voltage of 6 V was applied to the three samples at $t = 0$. (b) Cumulative BBG release of two other samples. They were differentiated from each other by the concentration of hydrogel beads used in the outer flow of the co-electrospray process (given in the plot). The dc voltage of 6 V was applied to the two samples at $t = 0$.

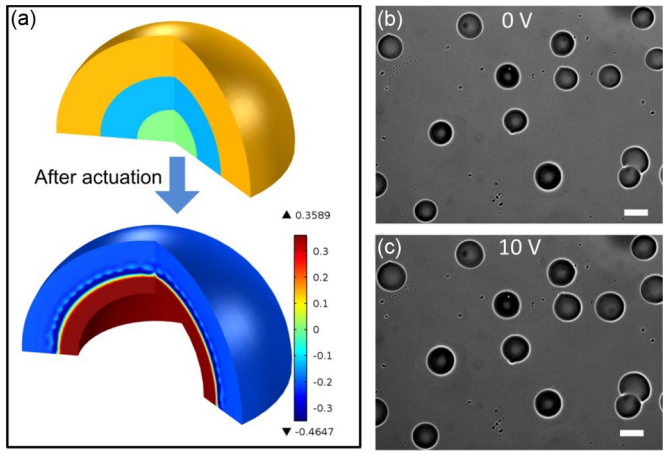

Fig. 7. (a) Simulation result of the deformation of a microcapsule (upper panel) before and (lower panel) after a stimulus. The color scale in the actuated state indicates the distribution of pressure, normalized by the elastic modulus of the polymer shell. The hydrogel bead was removed to show the deformed structure (the pressure in the gel core was identical to that in the liquid layer). It was assumed that the volume occupied by each water molecule in hydrogel gel was larger than that in liquid water. The swelling of the hydrogel bead caused the volume increase of the water–hydrogel system inside and consequently the expansion of the entire microcapsule. (b) and (c) Optical images showing the increase in the OD of the microcapsules (ID $= 16.5 \pm 3.5$ μm, $T_{\rm shell} = 5.1 \pm 2.8$ μm, and $C_{\rm bead} = 2 \times 10^8$/mL) at applied dc voltages of 0 and 10 V, respectively. The scale bars represent 20 μm.

interesting to point out that, after the initial release, no obvious difference was observed in the cumulative release with time between the three samples. We believe that the reason is the following: Since the OD of the microcapsules in the three samples was the same, their ID had the relationship of $\mathrm{ID_{S1}} > \mathrm{ID_{S2}} > \mathrm{ID_{S3}}$. The volume expansion of the hydrogel beads in the different samples was the same under the same voltage condition. This caused the internal pressure increase ΔP inside the microcapsules of the three samples to have the relationship of $\Delta P_{\rm S1} < \Delta P_{\rm S2} < \Delta P_{\rm S3}$. Thus, the influence of decreasing the shell thickness on the release rate of the encapsulated molecules was largely counteracted by that of decreasing the internal pressure of the microcapsules. On the other hand, to demonstrate controlling the molecule release by changing the quantity of the hydrogel beads inside the microcapsules, two other samples (named samples $\mathrm{N_1}$ and $\mathrm{N_2}$) were prepared by using $C_{\rm bead} = 2 \times 10^7$/mL for $\mathrm{N_1}$ and $C_{\rm bead} = 2 \times 10^8$/mL for $\mathrm{N_2}$ [see Fig. 6(b)]. Both samples had the same $T_{\rm shell} = 5.1 \pm 2.8$ μm and ID $= 16.5 \pm 3.5$ μm. The dc voltage of 6 V was applied to the samples at $t = 0$. Because sample $\mathrm{N_2}$ included more hydrogel beads than sample $\mathrm{N_1}$, the initial release from $\mathrm{N_2}$ ($t_{\rm N2} = 32$ min) was detected earlier than that from $\mathrm{N_1}$ ($t_{\rm N1} = 48$ min). Over the period of ~40 min after the initial release, the cumulative release from sample $\mathrm{N_1}$ was 10.4 ± 1.51%, which was less than that from $\mathrm{N_2}$ of 13.34 ± 1.75%. Afterward, the release curves of the two samples had a similar changing tendency with time. Similarly, this was because after that 40-min period, the molecule release in both samples was driven only by regular diffusion.

IV. Discussion

To elucidate the underlying release mechanism of the present microcapsules, we constructed a model of the tri-layer core–shell structure and carried out a numerical simulation of the swelling process after a stimulus. According to the experimental result shown in Fig. 7(b) and (c), the OD of the microcapsules (ID $= 16.5 \pm 3.5$ μm, $T_{\rm shell} = 5.1 \pm 2.8$ μm, and $C_{\rm bead} = 2 \times 10^8$/mL) increased by 8.5% as we increased the applied dc voltage from 0 to 10 V. Thus, the total volume of the hydrogel beads–solution system inside of the microcapsules increased as the hydrogel absorbed water. Given the low permeability of the PDLA shell, the volume increase was likely caused by the positive excess volume when mixing water and polymer in the hydrogel, as has been observed in similar systems [35]. The positive excess volume may be related to voids in the gels or to the different spatial arrangement of water molecules in the gels. To account for such an effect, we modified the classic Flory–Rehner theory [48], [49], by assuming that each water molecule occupied a volume twice as large as the volume it occupies in a pure liquid phase. The static behavior of the liquid layer was modeled by an incompressible solid of negligible shear modulus, with its volume decreasing as the gel core swelled. The outer PDLA shell was modeled as a neo-Hookean solid with an elastic modulus three orders of magnitude higher than that of the hydrogel when dry.

For illustration purposes, we took the representative values of the experiments and set the initial diameter ratio of the gel core, liquid layer, and PDLA shell as 1 : 2 : 3.2, as shown in Fig. 7(a). Although, in the experiments, each microcapsule often contained different numbers of hydrogel beads [see Fig. 2(h)], in the simulation, we lumped the volume of multiple beads into one to maintain a simple symmetric structure. As the actuation mechanism was coupled through a liquid layer, the actual shape and number of the gel beads should not affect the overall volume expansion. The gel core was initially in equilibrium with the liquid water. To model the effect of the stimulus, we reduced the Flory–Huggins parameter from 0.5 to −0.1. Such a change made the hydrogel more hydrophilic, so that it would take in more water and swell. The parameters were chosen so that the hydrogel beads increased in diameter approximately by a factor of 2 when unconstrained, as shown in Fig. 3. Inside the liquid-filled microcapsule, the bead swells at the expense of the water from the liquid layer. The positive excess volume

caused the bead–liquid system to expand, resulting in a $\sim$8% increase in the diameter of the microcapsule and an increased pressure in the liquid layer, as shown in Fig. 7(a) (lower panel). The calculated increase in the diameter was comparable with that observed in Fig. 7(b) and (c). Taking a representative value for the modulus of PDLA, which is $\sim$2 GPa, we estimated the peak internal pressure to be $\sim$600 MPa. For molecules of size $\sim 10^{-28}$ m^3, the internal pressure provided a chemical potential of $\sim 10\, k_{\mathrm{B}}T$, which was much higher than the entropic driving force of regular diffusion and thus dominated the release process. Other than the significantly increased driving force, the strain in the shell could also have increased the porosity and, consequently, the permeability of PDLA. However, we believe that compared with the increased internal pressure, the permeability change of PDLA was a relatively minor factor (due to the $\sim$8% increase in the OD) in the experiment. To date, it was technically difficult to examine the pore size change of the PDLA shells with surrounding liquids. Nevertheless, the observed increase in the OD resulted from the increased internal pressure of the liquid core, which could dominate the release process of the microcapsules.

It is known that degradation behaviors of PDLA are generally affected depending on the molecular weight (MW) of raw polymers used [50]. Previous research demonstrated that low-MW (e.g., 17 000) PDLA microstructures exhibited significant degradation and water hydration in the low-MW PDLA microstructures, whereas high-MW (e.g., 41 000) microstructures showed slight detectable degradation (until 53 days) [50]. Since our microcapsules used the high-MW PDLA $(\mathrm{MW} = 41\,000)$ as the shell polymer, we believe that the influence of the polymer degradation on the release profile of the encapsulated molecules was negligibly small.

There are several issues that remain. The distribution of hydrogel beads inside the microcapsules followed the Poisson distribution with relatively low uniformity. In addition, the size of our homemade hydrogel beads was not uniform either. To realize a more accurate and reliable release system, it is necessary to investigate how to prepare uniform-sized hydrogel beads and disturb the natural Poisson distribution of the beads inside the microcapsules in the future. We note that the incorporation of the hydrogel beads into the interior of the microcapsules reduced the actual molecule loading capacity of the microcapsules. In addition, hydrogel beads may absorb some of the encapsulated molecules. It is believed that optimization of the microcapsule dimensions and the hydrogel chemistry can minimize the loading and release yield issues. Furthermore, the electrically sensitive hydrogel used in this work expanded with an increased voltage, causing an earlier and faster release of molecules from the microcapsules. However, by engineering a hydrogel capable of shrinking with an increased voltage, it might be possible to delay the release of molecules from the microcapsules. In addition, the PDLA polymer and the BBG dye were used as a model material combination for the polymeric shell and the releasable molecule, respectively, in the present microcapsules. This material combination led to the controlled molecule delivery in a relatively short time since the natural diffusion-based release of BBG from the PDLA shell was already quite fast. However, it is rational to expect that, by employing an appropriate shell polymeric material (e.g., initial pore size, shell thickness, etc.) and releasable molecules (e.g., molecule weight, size, etc.), we probably will be able to obtain microcapsules for long-term drug delivery applications.

Because it would be fairly challenging to electrically stimulate the microcapsules in a human body, the present microcapsule technology with the embedded electrically sensitive hydrogel beads may not be suitable for *in vivo* drug delivery applications. However, it should be pointed out that the electrically sensitive hydrogel was used as a model material of internal bead actuators. There are many other types of hydrogel sensitive to *relatively* biologically friendly stimuli such as infrared radiation [41], [42], ultrasound [43], and magnetic fields [44]. These electromagnetic fields have been used in various medical applications. Therefore, by incorporating the corresponding hydrogel beads into the liquid core of the microcapsules via the co-electrospray technique, it is possible to apply the present controlled release mechanism to *in vivo* drug delivery applications in the future. Currently, the microcapsules with infrared-, ultrasound-, and magnetic-field-sensitive hydrogel beads are under development. We can envision that, instead of being exposed to electric fields, these new microcapsules can be exposed to their corresponding stimulation source such as infrared diode, ultrasound generator, and magnetic field generator. Similarly, the releasable molecules preloaded in the liquid core of the microcapsules can be released out of the polymer shell via the internal pressure regulation of the hydrogel beads in response to a specific external stimulation. There, of course, will be a lot of efforts to investigate the workability of these new microcapsules under medically safe doses of different electromagnetic fields.

Finally, the internal actuation approach presented in this paper could be potentially applied to many other existing controlled release mechanisms (e.g., shell rupture, shell dissolving by enzyme attract or chemical reaction, and stimuli-responsive shell), having a broad impact on controlled encapsulation and release of biological and chemical agents and species (e.g., drugs, proteins, vitamins, cells, fragrances, and flavors) that are important to many applications ranging from food and pharmaceutical industry to inkless paper.

V. Conclusion

We have developed the MEMS-like liquid core–polymer shell microcapsules with embedded electrically sensitive hydrogel beads. The microcapsules were able to regulate the release profile of the encapsulated BBG molecules, by using external electric fields. The microcapsules were fabricated using a simple and single-step co-electrospray process. The statistical distribution of the number of hydrogel beads embedded in the microcapsules was adjusted by changing the concentration of the hydrogel beads in the inner flow of the co-electrospray process. The ID of the microcapsules increased as the inner flow rate increased. We have also demonstrated that the BBG molecule release from the microcapsules started earlier for higher applied voltages. Additionally, higher applied voltages triggered the release of larger numbers of encapsulated molecules during the first several dozen minutes after the initial

release. Furthermore, decreasing the shell thickness of the microcapsules caused an earlier initial release, while having little influence on the release rate (given that the OD of the microcapsules was fixed). Finally, increasing the number of hydrogel beads in the microcapsules resulted in not only an earlier initial release but also a faster release during a 40-min period after the initial release. Due to the limited scope of this paper, this paper did not present a specific application to show the usefulness of controlled release of molecules from our microcapsules. However, generally, a controlled release is beneficial in the sense that it allows regulating the release profile of molecules over time, which otherwise would just follow a natural release profile (often determined by the material property of polymeric capsules). The results given in Figs. 4–6 have demonstrated that our microcapsules possessed this capability. It is believed that this novel core–shell microcapsule technology can potentially be a valuable addition to the area of controlled molecule release in general. A demonstration of controlled release of pharmacologically important molecules via a biologically friendly stimulation method (e.g., ultrasound, infrared radiation, and magnetic field) will be reported in the future.

ACKNOWLEDGMENT

The authors would like to thank the members of the Nano-Electro-Mechanical-Systems and Lab-on-Chip Laboratory for the helpful discussion.

REFERENCES

[1] C. Wang, Q. Ge, D. Ting, D. Nguyen, H.-R. Shen, J. Chen, H. N. Eisen, J. Heller, R. Langer, and D. Putnam, "Molecularly engineered poly(ortho ester) microspheres for enhanced delivery of DNA vaccines," *Nat. Mater.*, vol. 3, no. 3, pp. 190–196, Mar. 2004.

[2] G. Orive, R. M. Hernandez, A. R. Gascon, R. Calafiore, T. M. S. Chang, P. de Vos, G. Hortelano, D. Hunkeler, I. Lacik, A. M. J. Shapiro, and J. L. Pedraz, "History, challenges and perspectives of cell microencapsulation," *Trends Biotechnol.*, vol. 22, no. 2, pp. 87–92, Feb. 2004.

[3] T. Wang, I. Lacik, M. Brissova, A. V. Anilkumar, A. Prokop, D. Hunkeler, R. Green, K. Shahrokhi, and A. C. Powers, "An encapsulation system for the immunoisolation of pancreatic islets," *Nat. Biotechnol.*, vol. 15, no. 4, pp. 358–362, Apr. 1997.

[4] N. C. Bigall, A. Curcio, M. P. Leal, A. Falqui, D. Palumberi, R. Di Corato, E. Albanesi, R. Cingolani, and T. Pellegrino, "Magnetic nanocarriers with tunable pH dependence for controlled loading and release of cationic and anionic payloads," *Adv. Mater.*, vol. 23, no. 47, pp. 5645–5650, Dec. 2011.

[5] H. N. Yow and A. F. Routh, "Formation of liquid core–polymer shell microcapsules," *Soft Matter*, vol. 2, no. 11, pp. 940–949, Oct. 2006.

[6] R. Atkin, P. Davies, J. Hardy, and B. Vincent, "Preparation of aqueous core/polymer shell microcapsules by internal phase separation," *Macromolecules*, vol. 37, no. 21, pp. 7979–7985, Oct. 2004.

[7] K. Wygladacz, N. Ye, C. Xu, W. Retter, M. Bell, A. Hilgenbrink, and E. Bakker, "Uniform polymeric hollow microcapsules with controlled doping levels fabricated under nonreactive conditions," *Adv. Mater.*, vol. 19, no. 8, pp. 1059–1063, Apr. 2007.

[8] J. Wang, L. Sun, K. Mpoukouvalas, K. Lienkamp, I. Lieberwirth, B. Fassbender, E. Bonaccurso, G. Brunklaus, A. Muehlebach, T. Beierlein, R. Tilch, H.-J. Butt, and G. Wegner, "Construction of redispersible polypyrrole core–shell nanoparticles for application in polymer electronics," *Adv. Mater.*, vol. 21, no. 10/11, pp. 1137–1141, Mar. 2009.

[9] Y. Zhao and L. Jiang, "Hollow micro/nanomaterials with multilevel interior structures," *Adv. Mater.*, vol. 21, no. 36, pp. 3621–3638, Sep. 2009.

[10] A. D. Dinsmore, M. F. Hsu, M. G. Nikolaides, M. Marquez, A. R. Bausch, and D. A. Weitz, "Colloidosomes: Selectively permeable capsules composed of colloidal particles," *Science*, vol. 298, no. 5595, pp. 1006–1009, Nov. 2002.

[11] D. O. Grigoriev, T. Bukreeva, H. Mohwald, and D. G. Shchukin, "New method for fabrication of loaded micro- and nanocontainers: Emulsion encapsulation by polyelectrolyte layer-by-layer deposition on the liquid core," *Langmuir*, vol. 24, no. 3, pp. 999–1004, Feb. 2008.

[12] M. Kobaslija and D. T. McQuade, "Polyurea microcapsules from oil-in-oil emulsions via interfacial polymerization," *Macromolecules*, vol. 39, no. 9, pp. 6371–6375, Sep. 2006.

[13] A. Shulkin and H. D. H. Stover, "Photostimulated phase separation encapsulation," *Macromolecules*, vol. 36, no. 26, pp. 9836–9839, Dec. 2003.

[14] A. M. Schmidt, "The synthesis of magnetic core–shell nanoparticles by surface-initiatied ring-opening polymerization of epsilon-caprolactone," *Macromol. Rapid Commun.*, vol. 26, no. 2, pp. 93–97, 2005.

[15] A. V. Korobko, W. Jesse, and J. R. C. van der Maarel, "Encapsulation of DNA by cationic diblock copolymer vesicles," *Langmuir*, vol. 21, no. 1, pp. 34–42, Jan. 2005.

[16] R. K. Shah, J.-W. Kim, J. J. Agresti, D. A. Weitz, and L.-Y. Chu, "Fabrication of monodisperse thermosensitive microgels and gel capsules in microfluidic devices," *Soft Matter*, vol. 4, no. 12, pp. 2303–2309, Nov. 2008.

[17] H. Zhao, J. F. Chen, Y. Zhao, L. Jiang, J. W. Sun, and J. Yun, "Hierarchical assembly of multilayered hollow microspheres from an amphiphilic pharmaceutical molecule of azithromycin," *Adv. Mater.*, vol. 20, no. 19, pp. 3682–3686, Oct. 2008.

[18] D. Lensen, D. M. Vriezema, and J. C. M. van Hest, "Polymeric microcapsules for synthetic applications," *Macromol. Biosci.*, vol. 8, no. 11, pp. 991–1005, Nov. 2008.

[19] S. F. M. van Dongen, H.-P. M. de Hoog, R. J. R. W. Peters, M. Nallani, R. J. M. Nolte, and J. C. M. van Hest, "Biohybrid polymer capsules," *Chem. Rev.*, vol. 109, no. 11, pp. 6212–6274, Nov. 2009.

[20] D. G. Shchukin, D. A. Gorin, and H. Mohwald, "Ultrasonically induced opening of polyelectrolyte microcontainers," *Langmuir*, vol. 22, no. 17, pp. 7400–7404, Aug. 2006.

[21] B. Radt, T. A. Smith, and F. Caruso, "Optically addressable nanostructured capsules," *Adv. Mater.*, vol. 16, no. 23/24, pp. 2184–2189, Dec. 2004.

[22] H. R. Bhagat, R. W. Mendes, E. Mathiowitz, and H. N. Bhargava, "Kinetics and mechanism of drug release from calcium alginate membrane coated tablets," *Drug Develop. Ind. Pharm.*, vol. 20, no. 3, pp. 387–394, Jan. 1994.

[23] B. P. Timko, T. Dvir, and D. S. Kohane, "Remotely triggerable drug delivery systems," *Adv. Mater.*, vol. 22, no. 44, pp. 4925–4943, Nov. 2010.

[24] A. Shaviv, S. Raban, and E. Zaidel, "Modeling controlled nutrient release from polymer coated fertilizers: Diffusion release from single granules," *Environ. Sci. Technol.*, vol. 37, no. 10, pp. 2251–2256, May 2003.

[25] D. J. Gan and L. A. Lyon, "Tunable swelling kinetics in core–shell hydrogel nanoparticles," *J. Amer. Chem. Soc.*, vol. 123, no. 31, pp. 7511–7517, Aug. 2001.

[26] K. N. Plunkett and J. S. Moore, "Patterned dual pH-responsive core–shell hydrogels with controllable swelling kinetics and volumes," *Langmuir*, vol. 20, no. 16, pp. 6535–6537, Aug. 2004.

[27] I. Tokarev and S. Minko, "Stimuli-responsive porous hydrogels at interfaces for molecular filtration, separation, controlled release, and gating in capsules and membranes," *Adv. Mater.*, vol. 22, no. 31, pp. 3446–3462, Aug. 2010.

[28] S. Murdan, "Electro-responsive drug delivery from hydrogels," *J. Control. Release*, vol. 92, no. 1/2, pp. 1–17, Sep. 2003.

[29] D. Li and Y. Xia, "Electrospinning of nanofibers: Reinventing the wheel?" *Adv. Mater.*, vol. 16, no. 14, pp. 1151–1170, Jul. 2004.

[30] Z. Y. Liu, D. D. Sun, and J. O. Leckie, "An efficient bicomponent TiO2/SnO2 nanofiber photocatalyst fabricated by electrospinning with a side-by-side dual spinneret method," *Nano Lett.*, vol. 7, no. 4, pp. 1081–1085, Apr. 2007.

[31] Z. C. Sun, A. L. E.Zussman, J. H. Yarin, and A. Wendorff, "Compound core–shell polymer nanofibers by co-electrospinning," *Adv. Mater.*, vol. 15, no. 22, pp. 1929–1932, Nov. 2003.

[32] Y. Zhao, X. Y. Cao, and L. Jiang, "Bio-mimic multichannel microtubes by a facile method," *J. Amer. Chem. Soc.*, vol. 129, no. 4, pp. 764–765, Jan. 2007.

[33] H. Y. Chen, Y. Zhao, Y. L. Song, and L. Jiang, "One-step multicomponent encapsulation by compound-fluidic electrospray," *J. Amer. Chem. Soc.*, vol. 130, no. 25, pp. 7800–7801, Jun. 2008.

[34] M. J. Bassetti, A. N. Chatterjee, N. R. Aluru, and D. J. Beebe, "Development and modeling of electrically triggered hydrogels for microfluidic applications," *J. Microelectromech. Syst.*, vol. 14, no. 5, pp. 1198–1207, Oct. 2005.

[35] L. Dong, A. K. Agarwal, D. J. Beebe, and H. Jiang, "Adaptive liquid microlenses activated by stimuli-responsive hydrogels," *Nature*, vol. 442, no. 7102, pp. 551–554, Aug. 2006.
[36] N.-C. Tsai and C.-Y. Sue, "Review of MEMS-based drug delivery and dosing systems," *Sens. Actuators A, Phys.*, vol. 134, no. 2, pp. 555–564, Mar. 2007.
[37] H. Yang, C. R. Lightner, and L. Dong, "Light-emitting coaxial nanofibers," *ACS Nano*, vol. 6, no. 1, pp. 622–628, Jan. 2012.
[38] R. Steendam, M. J. van Steenbergen, W. E. Hennink, H. W. Frijlink, and C. F. Lerk, "Effect of molecular weight and glass transition on relaxation and release behaviour of poly(DL-lactic acid) tablets," *J. Control. Release*, vol. 70, no. 1/2, pp. 71–82, Jan. 2001.
[39] Y. S. Jo, D. K. Kim, Y. K. Jeong, K. J. Kim, and M. Muhammed, "Encapsulation of bovine serum albumin in temperature-programmed 'shell-in-shell' structures," *Macromol. Rapid Commun.*, vol. 24, no. 16, pp. 957–962, Nov. 2003.
[40] H. Yang, W. Hong, and L. Dong, "A controlled biochemical release device with embedded nanofluidic channels," *Appl. Phys. Lett.*, vol. 100, no. 15, pp. 153510-1–153510-4, Apr. 2012.
[41] X. Zeng and H. Jiang, "Tunable liquid microlens actuated by infrared light-responsive hydrogel," *Appl. Phys. Lett.*, vol. 93, no. 15, pp. 151101-1–151101-3, Oct. 2008.
[42] A. Suzuki and T. Tanaka, "Phase transition in polymer gels induced by visible light," *Nature*, vol. 346, no. 6282, pp. 345–347, Jul. 1990.
[43] D. Troiani, J. R. Dion, and D. H. Burns, "Ultrasonic quantification using smart hydrogel sensors," *Talanta*, vol. 83, no. 5, pp. 1371–1375, Feb. 2011.
[44] M. Namdeo, S. K. Bajpai, and S. Kakkar, "Preparation of a magnetic-field-sensitive hydrogel and preliminary study of its drug release behavior," *J. Biomater. Sci. Polym. Ed.*, vol. 20, no. 12, pp. 1747–1761, Jan. 2009.
[45] J. F. Edd, D. Di Carlo, K. J. Humphry, S. Koster, D. Irimia, D. A. Weitz, and M. Toner, "Controlled encapsulation of single-cells into monodisperse picolitre drops," *Lab Chip*, vol. 8, no. 8, pp. 1262–1264, Aug. 2008.
[46] H. Yang, X. Qiao, M. K. Bhattacharyya, and L. Dong, "Microfluidic droplet encapsulation of highly motile single zoospores for phenotypic screening of an antioomycete chemical," *Biomicrofluidics*, vol. 5, no. 4, pp. 044103-1–044103-11, Dec. 2011.
[47] T. Higuchi, "Mechanism of sustained-action medication: Theoretical analysis of rate of release of solid drugs dispersed in solid matrices," *J. Pharm. Sci.*, vol. 52, no. 12, pp. 1145–1149, Dec. 1963.
[48] P. J. Flory and J. Rehner, "Statistical mechanics of cross linked polymer networks II. Swelling," *J. Chem. Phys.*, vol. 11, no. 11, pp. 521–526, Nov. 1943.
[49] W. Hong, X. Zhao, J. Zhou, and Z. Suo, "A theory of coupled diffusion and large deformation in polymeric gels," *J. Mech. Phys. Solids*, vol. 56, no. 5, pp. 1779–1793, May 2008.
[50] T. G. Park, "Degradation of poly(d, l-lactic acid) microspheres: Effect of molecular weight," *J. Control. Release*, vol. 30, no. 2, pp. 161–173, May 1994.

Haifeng Yang received the B.S. degree in biomedical engineering from Tianjin University, Tianjin, China, in 2007. He was a graduate student in biomedical engineering at the University of Texas Southwestern Medical Center at Dallas from 2007 to 2008. He is currently working toward the Ph.D. degree in the Department of Electrical and Computer Engineering, Iowa State University, Ames.

His research interests include the development of micro/nanofibers and particles for controlled delivery of biomolecules and microfluidic lab-on-chips.

Xuan Qiao is currently a senior undergraduate student in the Department of Electrical and Computer Engineering, Iowa State University, Ames.

He joined Dr. Liang Dong's research laboratory as an Undergraduate Researcher in 2011.

Wei Hong received the B.S. degrees in engineering mechanics and computer science and engineering and the M.S. degree in solid mechanics from Tsinghua University, Beijing, China, in 2000 and 2002, respectively, and the Ph.D. degree in engineering sciences from Harvard University, Cambridge, MA, in 2006.

He was a Postdoctoral Research Fellow with the School of Engineering and Applied Sciences, Harvard University, between 2006 and 2008. Since 2008, he has been an Assistant Professor with the Department of Aerospace Engineering, Iowa State University, Ames, where he also holds courtesy appointments in the Department of Materials Science and Engineering and the Department of Mechanical Engineering. His current research interest focuses on the multiphysics modeling of materials and structures, particularly soft and smart material systems.

Liang Dong (M'03) received the B.S. degree in precision instruments from Xidian University, Xi'An, China, in 1999 and the Ph.D. degree in electronic science and technology from Tsinghua University, Beijing, China, in 2004.

From 2004 to 2007, he was a Postdoctoral Research Associate with the Department of Electrical and Computer Engineering, University of Wisconsin, Madison. Since 2007, he has been an Assistant Professor with the Department of Electrical and Computer Engineering, Iowa State University, Ames, where he is also a courtesy Assistant Professor with the Department of Chemical and Biological Engineering. He is also an Associate with the U.S. Department of Energy's Ames Laboratory, Ames. His research is focused on developing lab-on-chip devices, biomedical instruments, microelectromechanical and nanoelectromechanical systems devices, nanophotonics, and nanomaterials.

Dr. Dong was the recipient of the National Outstanding Doctoral Dissertation Award of China in 2007. He was also the recipient of the Warren B. Boast Undergraduate Teaching Award in 2010, the Harpole-Pentair Developing Faculty Award in 2010–2011 and 2011–2012, and the College of Engineering's Early Career Engineering Faculty Research Award in 2011, all at Iowa State University. He also received the National Science Foundation's CAREER Award in 2010.